Journal of Statistical Physics, Vol. 111, Nos. 1/2, April 2003 (© 2003)

The Percolation Transition for the Zero-Temperature Stochastic Ising Model on the Hexagonal Lattice

C. Douglas Howard[1] and Charles M. Newman[2]

Received October 24, 2001; accepted August 6, 2002

On the planar hexagonal lattice $\mathbb{H}$, we analyze the Markov process whose state $\sigma(t)$, in $\{-1, +1\}^{\mathbb{H}}$, updates each site v asynchronously in continuous time $t \geqslant 0$, so that $\sigma_v(t)$ agrees with a majority of its (three) neighbors. The initial $\sigma_v(0)$'s are i.i.d. with $P[\sigma_v(0) = +1] = p \in [0, 1]$. We study, both rigorously and by Monte Carlo simulation, the existence and nature of the percolation transition as $t \to \infty$ and $p \to 1/2$. Denoting by $\chi^+(t, p)$ the expected size of the plus cluster containing the origin, we (1) prove that $\chi^+(\infty, 1/2) = \infty$ and (2) study numerically critical exponents associated with the divergence of $\chi^+(\infty, p)$ as $p \uparrow 1/2$. A detailed finite-size scaling analysis suggests that the exponents γ and ν of this $t = \infty$ (dependent) percolation model have the same values, 4/3 and 43/18, as standard two-dimensional independent percolation. We also present numerical evidence that the rate at which $\sigma(t) \to \sigma(\infty)$ as $t \to \infty$ is exponential.

KEY WORDS: Glauber dynamics; dependent percolation; Ising spin dynamics; hexagonal lattice; critical exponents.

1. INTRODUCTION

Stochastic Ising models, a special class of interacting particle systems, are Markov processes $\sigma(t)$ with state space $\mathscr{S} \equiv \{-1, +1\}^{\mathbb{L}}$ where $\mathbb{L}$ is some regular lattice. They have been much studied in both the statistical physics and probability theory literature (see, e.g., refs. 1 and 2). Their physical and mathematical significance is tied to the fact that their transition probabilities/rates are chosen so that the Gibbs measures (for some Hamiltonian) at temperature T are invariant distributions for the Markov

[1] City University of New York–Baruch College, Box B6-230, One Bernard Baruch Way, New York, New York 10010; e-mail: dhoward@baruch.cuny.edu.

[2] Courant Institute of Mathematical Sciences, New York University, 251 Mercer Street, New York, New York 10012; e-mail: newman@courant.nyu.edu

0022-4715/03/0400-0057/0

process. In systems where there are multiple (infinite-volume) Gibbs measures for T below some critical T_c, a subject of considerable interest is the $t \to \infty$ behavior of $\sigma(t)$ (with temperature $T = T_1 < T_c$) when the initial state is chosen from the (unique) Gibbs measure at $T = T_2 > T_c$. In this paper, we study a continuous time stochastic Ising model with $\mathbb{L}$ the planar hexagonal lattice $\mathbb{H}$ and, as in much of the statistical physics literature (see, e.g., ref. 1), we focus on the limiting case where $T_1 = 0$ and $T_2 = \infty$. (Some interesting results for a natural discrete time process on $\mathbb{H}$ may be found in ref. 3.)

Our $T_1 = 0$ continuous time process $\sigma(t)$ for $t \geqslant 0$, related to the Hamiltonian for the homogeneous ferromagnetic Ising model on $\mathbb{H}$, may be defined in terms of rate-one Poisson processes (independent for different vertices v)—which we think of as rings of Poisson "clocks." When the clock at v rings at time $t^* > 0$, the spin $\sigma_v(t^*)$ flips (i.e., $\sigma_v(t^*+) = -\sigma_v(t^*)$) if and only if $\sigma_v(t^*)$ agrees with a minority (here, at most one) of its three neighboring spins at time t^*. The ($T_2 = +\infty$) initial distribution for $\sigma(0) \equiv (\sigma_v(0) : v \in \mathbb{H})$ corresponds to i.i.d. $\sigma_v(0)$'s; we allow for a bias parameter $p = P[\sigma_v(0) = +1] \in [0, 1]$.

We will denote by $P_{t,p}$, for $t \geqslant 0$ and $p \in [0, 1]$, the probability distribution on $\mathscr{S}$ of $\sigma(t)$ in this Markov process; we denote by $E_{t,p}$ expectation with respect to $P_{t,p}$. We note that $P_{t,p}$ is also well defined for $t = \infty$, since, as a corollary of a general theorem of Nanda *et al.*,[4] almost surely each spin σ_v flips only finitely many times, thereby ensuring the existence of the $t \to \infty$ limiting configuration $\sigma(\infty)$; $P_{\infty,p}$ is then the distribution of this $\sigma(\infty)$.

In this paper, we study the site percolation properties of (say) the $+1$ sites. Unless otherwise explicitly stated, all critical probabilities refer to site percolation on $\mathbb{H}$ of $\sigma(t)$. Let $\mathscr{C}_v^+$ denote the plus cluster of site $v \in \mathbb{H}$, let 0 denote some specified "origin" site in $\mathbb{H}$, and let $\theta(t, p) = P_{t,p}[|\mathscr{C}_v^+| = \infty] = P_{t,p}[|\mathscr{C}_0^+| = \infty]$, where $|\cdot|$ denotes cardinality, and $\chi^+(t, p) = E_{t,p}[|\mathscr{C}_v^+|] = E_{t,p}[|\mathscr{C}_0^+|]$. We define the critical probability as $p_c(t) \equiv \inf\{p : \chi^+(t, p) = \infty\}$. This definition is reasonable since each $\sigma_v(t)$ is stochastically increasing in the time 0-spin configuration and hence, for any fixed t, χ^+ is increasing in p. Of course, for $t = 0$, $P_{0,p}$ is simply a product measure describing independent site percolation on $\mathbb{H}$, where $p_c(0)(\approx 0.7) > 1/2$ [ref. 5, p. 275]; thus $\chi^+(0, p) < \infty$ and $\theta(0, p) = 0$ (i.e., there is no percolation) if $p < p_c(0)$. For $t > 0$, $P_{t,p}$ describes a *dependent* percolation process for which relatively little is known. The purpose of this paper is to provide some evidence, both rigorous and numerical, about the existence and nature of a percolation transition at $t = \infty$, $p = 1/2$.

It is rather easy to show (we leave it as an exercise) that for $p < p_c(0)$ and then small t (how small depends on p), the system is subcritical in that, e.g., $\chi^+(t, p) < \infty$. It is also known (see refs. 3 and 6, where this is shown, respectively for $\mathbb{L}=\mathbb{H}$ and $\mathbb{L}=\mathbb{Z}^2$, by combining old results of Harris[7] and of Gandolfi *et al.*[8]) that there is no percolation for $p=1/2$ for any t, including $t=\infty$; i.e., $\theta(t, 1/2)=0$ for any $t\in[0,\infty]$. The main rigorous result of this paper, presented in Section 2, is a proof that $\chi^+(\infty, 1/2)=\infty$; we conjecture that $\chi^+(t, 1/2)<\infty$ for any $t<\infty$ which would imply the existence of a percolation transition as $t\to\infty$ at $p=1/2$.

We also conjecture that at $t=\infty$, $\chi^+(\infty, p)<\infty$ for $p<1/2$ so that the $t=\infty$, $p=1/2$ critical point would exhibit a transition from another direction in the (t, p) plane. This conjecture will be supported by numerical evidence concerning the nature of the divergence of $\chi^+(\infty, p)$ as $p\uparrow 1/2$. Indeed, a major part of this paper will be a detailed analysis, presented in Section 3, of simulation data about two critical exponents, γ and ν, associated with this divergence. Our conclusion is that $\gamma=4/3$ and $\nu=43/18$, the well known values for two-dimensional *independent* percolation[9–11] (for other references, see ref. 12, p. 279).

2. INFINITE EXPECTED CLUSTER SIZE AT $t=\infty$, $p=1/2$

We represent $\mathbb{H}$ as a graph embedded in $\mathbb{R}^2$ with vertex set $\mathbb{V}=\bigcup_{i,j\in\mathbb{Z}}(\mathbb{V}_0+i\mathbf{u}+j\mathbf{v})$, where

$$\mathbb{V}_0=\left\{\left(\frac{\sqrt{3}}{2},\frac{1}{2}\right),(0,1),\left(-\frac{\sqrt{3}}{2},\frac{1}{2}\right),\left(\frac{-\sqrt{3}}{2},\frac{-1}{2}\right),(0,-1),\left(\frac{\sqrt{3}}{2},\frac{-1}{2}\right)\right\},\tag{1}$$

$\mathbf{u}=(\sqrt{3},0)$ and $\mathbf{v}=(\frac{\sqrt{3}}{2},\frac{3}{2})$. The edge set $\mathbb{E}$ consists of all pairs of vertices $\{u, v\}$ from $\mathbb{V}$ with the Euclidean distance $\|u-v\|$ from u to v equal to 1; we identify the segment $\overline{uv}$ with the edge $\{u, v\}$.

A cell of $\mathbb{H}$ will mean any of the closed subsets of $\mathbb{R}^2$ whose boundary consists of six consecutive edges of $\mathbb{H}$ obtained by always turning, say, clockwise. If $\mathscr{H}$ is any finite collection of cells and $R\equiv\bigcup_{C\in\mathscr{H}}C$ is simply connected, we let ∂R denote the Jordan curve that is R's boundary in $\mathbb{R}^2$. For vertices a and b on ∂R, $\partial_a^b R$ denotes the portion of ∂R going clockwise from a to b. If A and B are subsets of ∂R, a crosscut in R from A to B is a path π from some vertex in A to some vertex in B along the edges in $\mathbb{H}\cap R$ with the property that all the vertices along π have a common spin. If σ is any spin configuration on $\mathbb{H}$ and v is any vertex of $\mathbb{H}$, $\mathscr{C}_v=\mathscr{C}_v(\sigma)$ will denote the set of vertices in the $\sigma(v)$-spin cluster at v. We also put $X_v=X_v(\sigma)\equiv|\mathscr{C}_v(\sigma)|$.

Theorem 1. Fix $\mathscr{H}$ and R as above with R simply connected. Suppose σ is a metastable spin configuration on $\mathbb{H}$. If distinct vertices

$u, v, w, x \in \partial R$ are listed in clockwise direction around ∂R then either: (1) there is a crosscut in R from $\partial_u^v R$ to $\partial_w^x R$; or, (2) there is a crosscut in R from $\partial_v^w R$ to $\partial_x^u R$.

Proof. This can be proved directly on the lattice $\mathscr{H}$, but the argument (as in an early draft of this paper) is somewhat lengthy and, as pointed out to us by F. Camia, there is a simpler proof based on the partition of $\mathscr{H}$ into two sublattices, by $\mathscr{A}$ and $\mathscr{B}$, such that all neighbors in $\mathscr{H}$ of vertices of $\mathscr{A}$ belong to $\mathscr{B}$ and vice-versa. The set $\mathscr{A}$ (and similarly the set $\mathscr{B}$) is then turned into a graph by declaring two vertices of $\mathscr{A}$ to be neighbors if they have a common $\mathscr{H}$-neighbor vertex in $\mathscr{B}$. (We remark that although the term sublattice is in common usage in the statistical mechanics literature, these are not subgraphs of the original graph $\mathscr{H}$ since the edges in $\mathscr{A}$ and $\mathscr{B}$ are not edges in $\mathscr{H}$.)

Each of $\mathscr{A}$ and $\mathscr{B}$ is a triangular lattice, with each vertex having exactly six neighbors. Furthermore (and unlike on the lattice $\mathscr{H}$), if a finite subset D of a triangular lattice has no holes (i.e., the complement D^c of D consists of only a single infinite connected component), then $\partial^* D$, defined as the set of vertices in D^c that are neighbors of some vertex in D, is also connected. Next note that the vertices in ∂R alternate between $\mathscr{A}$ and $\mathscr{B}$ and that each of the four pieces of ∂R (which overlap at their endpoints) must contain at least one site of $\mathscr{A}$ (or else two of the vertices u, v, w, x coincide and the conclusion of the theorem is trivial).

Consider the subgraph G of $\mathscr{A}$ consisting of all the vertices in $R \cap \mathscr{A}$ (along with the edges between them). It is a standard fact about site percolation on the triangular lattice that there is either a plus-spin path in G from $G \cap \partial_u^v R$ to $G \cap \partial_w^x R$ or else a minus-spin path from $G \cap \partial_v^w R$ to $G \cap \partial_x^u R$. (To see this, let D be the union of the plus-clusters in G of those vertices in $G \cap \partial_u^v R$; if this does not touch $G \cap \partial_w^x R$, then the plus-cluster of $\partial^* D \cap G$ will be connected and touch both $G \cap \partial_v^w R$ and $G \cap \partial_x^u R$ so that it will contain the needed plus-path.)

The final step of the argument is to note that a (self-avoiding) constant-spin path in $\mathscr{A}$ from a metastable spin configuration on $\mathscr{H}$ contains a sub-path (with the original two endpoints from $\mathscr{A}$) so that the interpolating vertices from $\mathscr{B}$ are all distinct and furthermore have that same spin value. Thus one obtains a (self-avoiding) constant-spin path in $\mathscr{H}$ between the original endpoints. ∎

Regarding expected cluster size, we have the following consequence of Theorem 1.

Theorem 2. Let μ be any measure on spin configurations on $\mathbb{H}$ that is concentrated on metastable configurations and is invariant with respect to all translations of $\mathbb{H}$. Then $E^{\mu}X_0 = \infty$. In particular, if μ is the distribution of $\sigma(\infty)$ corresponding to any $p \geqslant 0.5$, then $EX_0^+ = \infty$.

Proof. This theorem follows from the proof of Theorem 1 combined with a result of Russo [ref. 13, Prop. 1] applied to the triangular sublattice $\mathscr{A}$ or $\mathscr{B}$ of $\mathbb{H}$. A direct proof along the same lines as in ref. 13 is as follows. Take the R of Theorem 1 to be R_ℓ, the union of the cells contained in an $\ell \times \ell$ square of $\mathbb{R}^2$ (with ℓ large) and let the u, v, w, x of Theorem 1 be near the four corners of the square. For each $z \in \partial R_\ell$, let A_z denote the event that there is a crosscut from z to (near) the opposite edge of the square, so that for some $c > 0$ and ℓ large, $X_z \geqslant c\ell$ if A_z occurs. By Theorem 1 and translation invariance, for some $b < \infty$,

$$b\ell\mu[X_0 \geqslant c\ell] \geqslant \sum_{z \in \partial R_\ell} \mu[A_z] \geqslant \mu\left[\bigcup_{z \in \partial R_\ell} A_z\right] = 1. \tag{2}$$

So for some $d > 0$, it follows that $\mu[X_0 \geqslant n] \geqslant d/n$ for $n \geqslant 1$ and

$$E^{\mu}[X_0] \geqslant \sum_{n=1}^{\infty} \mu[X_0 \geqslant n] \geqslant \sum_{n=1}^{\infty} d/n = \infty. \quad \blacksquare \tag{3}$$

3. SIMULATION METHODOLOGY AND MAIN RESULTS

For any positive integer L, define the vertex set $\mathbb{V}(L)$ by

$$\mathbb{V}(L) \equiv \bigcup_{0 \leqslant i, j < L} (\mathbb{V}_0 + i\mathbf{u} + j\mathbf{v}), \tag{4}$$

with $\mathbf{u}$ and $\mathbf{v}$ as given in the previous section of the paper. For various values of L, we numerically estimate several statistical properties of the process on finite lattice patches $\mathbb{V}^*(L)$, which are simply the $\mathbb{V}(L)$ with periodic boundary conditions. To implement the boundary conditions, $\mathbb{V}^*(L)$ is $\mathbb{V}(L)$ with sites v along the lower edge of the patch (see Fig. 1(a)) identified with sites $v + L\mathbf{v}$ and sites u along the left edge identified with sites $u + L\mathbf{u}$. Specifically, let $\mathbb{V}^*(L)$ denote $\mathbb{V}(L)$ with the vertices on the upper and rightmost "boundaries" deleted, so that $\mathbb{V}^*(L)$ eliminates the duplication in $\mathbb{V}(L)$ caused by identified sites. In Fig. 1(a), for example, where $L = 8$, the sites v, v' and v'' are all identified. The vertex set $\mathbb{V}^*(8)$ is represented by the •'s. Let $\mathbb{H}^*(L)$ denote the subgraph of $\mathbb{H}$ generated by the vertex set $\mathbb{V}^*(L)$, together with additional edges $\{u, v\}$ where (1) $u, v \in \mathbb{V}^*(L)$, and (2) for some $v' \in \mathbb{V}$, v' is identified with v and $\{u, v'\} \in \mathbb{E}$.

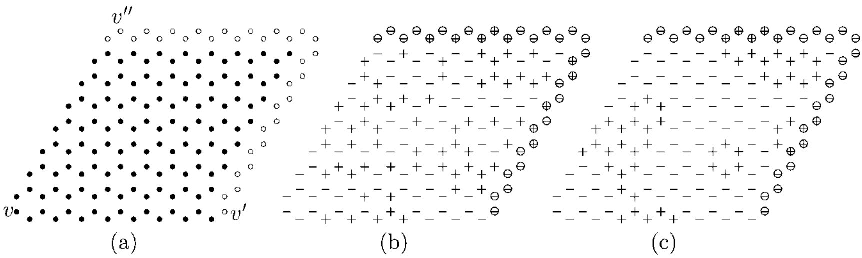

Fig. 1. (a) The finite lattice patch $V^*(8)$, (b) an initial configuration on $V^*(8)$, and (c) a possible resulting metastable configuration.

In addition to varying L, we also vary the parameter p that measures the (mean) density of $+1$ spins in the time 0 configuration This configuration, $(\sigma_v(0)\colon v \in \mathbb{V}^*(L))$, comprises i.i.d. ± 1-valued random variables satisfying $P[\sigma_v(0) = +1] = p$. Figure 1(b) shows an illustrative time 0 configuration on $\mathbb{V}^*(8)$.

To implement the dynamics, we randomly (i.e., uniformly, with replacement) select a sequence of sites from $\mathbb{V}^*(L)$. This sequencing varies from simulation to simulation and is independent of the $\sigma_v(0)$'s. When a site is selected, its spin is altered, if necessary, to come into agreement with a majority of its three neighbors. This proceeds until achieving a "metastable" configuration $(\sigma_v(\infty)\colon v \in \mathbb{H}^*(L))$, characterized by the fact that it is stable under the dynamics. Figure 1(c) shows a metastable configuration that corresponds to some realization of the dynamics applied to the configuration in Fig. 1(b).

When measuring the statistical properties corresponding to a given pair (p, L), we typically ran a large number of independent simulations. The time 0 spin configurations and the dynamics are constructed to be independent across all combinations of (p, L). For example, changing either one of p or L results in a completely independent simulated process. As stated above, the dynamics are independent of the time 0 configurations.

Phase Transition, Part 1. Here we numerically identify the value of $p_c(\infty)$ and the values of various critical exponents associated with this phase transition. In particular, the critical exponent $\gamma(t)$ is defined by the (infinite-volume) relation $\chi^+(t, p) \sim (p_c(t) - p)^{-\gamma(t)}$ as $p \uparrow p_c(t)$. Similarly, $v(t)$ denotes the correlation length exponent of the system at time t. (The correlation length $\xi^+ = \xi^+(t, p)$ may be defined by $P_{t,p}[v \in \mathscr{C}_u^+] \sim \exp(-\|u - v\|/\xi^+)$ as $\|u - v\| \to \infty$ and then $v(t)$ is defined by $\xi^+(t, p) \sim (p_c(t) - p)^{-v(t)}$ as $p \uparrow p_c(t)$.) At $t = 0$, $p_c(0) \approx 0.7$, and the critical exponents should have the usual two-dimensional values of $\gamma(0) = 43/18$ and

$\nu(0) = 4/3$ (although these are not yet completely rigorous). As we shall see, it turns out that $p_c(\infty) = 1/2$, but the critical exponents continue to have the usual values: $\gamma(\infty) = 43/18$ and $\nu(\infty) = 4/3$. In this Part 1, however, we treat $p_c(\infty)$ and the two exponent values as unknown quantities that we are trying to estimate. Although our approach in Part 1 is to estimate $p_c(\infty)$, $\gamma(\infty)$, and $\nu(\infty)$ simultaneously, other approaches, where $p_c(\infty)$ is estimated first, are possible—see, e.g., ref. 14. In Part 2, we will statistically test the hypothesis that $1/2, 43/18$, and $4/3$ are indeed the correct values.

Our basic approach is to study the behavior of $+1$ cluster sizes on finite lattice patches. To compute average $+1$ cluster size, we ran simulations for various values of L and p. For $v \in \mathbb{V}^*(L)$, let $X_v^+(p, L, n)$ denote the size of the $+1$ cluster (in $\mathbb{V}^*(L)$) at v at time ∞ (i.e., in the terminal metastable state) for the nth simulation, so $X_v^+(p, L, \cdot) = 0$ if $\sigma_v(\infty) = -1$ for that simulation. We computed the average cluster size for the nth simulation as

$$\bar{X}^+(p, L, n) = \frac{1}{|\mathbb{V}^*(L)|} \sum_{v \in \mathbb{V}^*(L)} X_v^+(p, L, n) = \frac{1}{|\mathbb{V}^*(L)|} \sum_{+1 \text{ clusters } \mathscr{C}} |\mathscr{C}|^2. \tag{5}$$

For Fig. 1(c), this calculation yields

$$\bar{X}^+ = \frac{1}{128}(6^2 + 38^2) = 11.5625. \tag{6}$$

(Note that in Fig. 1(c) there are only two $+1$ clusters, rather than the apparent four, because of the vertex identifications.) For each of many values of p and L, we ran 10,000 such simulations. We then estimated the expected cluster size for the finite system as

$$E\bar{X}^+(p, L) \approx \hat{X}^+(p, L) \equiv \frac{1}{10{,}000} \sum_n \bar{X}^+(p, L, n), \tag{7}$$

and further estimated the standard deviation, $\sigma(p, L)$, of the $\hat{X}^+$ estimator as

$$\sigma(p, L) \equiv \mathrm{Std}(\hat{X}^+(p, L)) \approx \hat{\sigma}(p, L)$$

$$\equiv \frac{1}{10{,}000} \sqrt{\sum_n (\bar{X}^+(p, L, n) - \hat{X}^+(p, L))^2}. \tag{8}$$

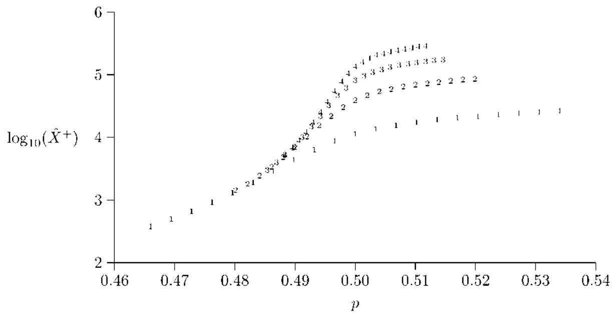

Fig. 2. $\log_{10}(\hat{X}^{+}(p, L))$ for (1) $L=200$, (2) $L=400$, (3) $L=600$, and (4) $L=800$.

We did this exercise for various values of p and for $L=200$, 400, 600, and 800. The results for $\hat{X}^{+}(p, L)$ are plotted in Fig. 2 and shown in tabular form along with their respective standard deviations in the Appendix.

We analyzed this data using finite-size scaling methods. Throughout the following we abbreviate $p_c^* = p_c(\infty)$, $\gamma^* = \gamma(\infty)$, and $\nu^* = \nu(\infty)$, representing the true values of the respective quantities. Symbols p_c, γ, and ν will represent "test" values of these quantities. According to the finite-size scaling ansatz, see, e.g., refs. 15–17, we should have, for $\gamma=\gamma^*$, $\nu=\nu^*$, $\delta=\delta^*$ (the exponent for the order of magnitude of the scaling error), and $p(s)=p_c+sL^{-1/\nu}$, that

$$E\bar{X}^{+}(p(s), L) = L^{\gamma/\nu}[f^*(s) + L^{-\delta}g^*(s) + \text{higher order terms}] \tag{9}$$

for some functions f^* and g^* that are independent of L. Of course, we do not know the quantities $E\bar{X}^{+}(p, L)$ or $\sigma(p, L)$, but rather have respectively the estimates $\hat{X}^{+}(p, L)$ and $\hat{\sigma}(p, L)$ for 21 values of p. With a sample size of 10,000, $\hat{X}^{+}(p, L)/\hat{\sigma}(p, L)$ should be approximately normal with variance one. For any numbers p_c, γ, ν, δ, and any functions f and g, error terms $\epsilon(p_c, \gamma, \nu, \delta, f, g; s, L)$ may be defined by the relation:

$$\frac{\hat{X}^{+}(p(s), L)}{\hat{\sigma}(p(s), L)} = \frac{L^{\gamma/\nu}}{\hat{\sigma}(p(s), L)} f(s) + \frac{L^{(\gamma/\nu)-\delta}}{\hat{\sigma}(p(s), L)} g(s) + \epsilon(p_c, \gamma, \nu, \delta, f, g\,; s, L). \tag{10}$$

Our model is that, for the correct p_c, γ, ν, δ, f, and g, the error term $\epsilon(p_c, \gamma, \nu, \delta, f, g\,; s, L)$ should be approximately a standard normal.

To estimate these four numerical quantities and two functions we would like to numerically search through p_c, γ, ν, δ, f and g with the objective of minimizing the sum

$$\sum_{s\in S}\sum_{L}\epsilon(p_c,\gamma,\nu,\delta,f,g\,;s,L)^2, \tag{11}$$

where $L=200$, 400, 600, and 800, and where s ranges over a fixed appropriate collection of values S. A difficulty that arises here is that the values $\{p(s)\colon s\in S\}$ depend on the value of p_c and ν (and on L, but this is not a difficulty). This is problematic because, for each of the four values of L, we have necessarily computed $\hat{X}^+(p,L)$ and $\hat{\sigma}(p,L)$ only for a limited number (i.e., 21) of values of p which are generally not those in $\{p(s)\colon s\in S\}$ (refer to (10)). (The values of p used, p_i^L for $0\leqslant i\leqslant 20$, depend on L—see Appendix.) To solve this, we fit polynomials, two for each value of L, to the 21 data points corresponding to $\hat{X}^+$ and $\hat{\sigma}$, i.e., to the points $(p_i^L,\hat{X}^+(p_i^L,L))_{0\leqslant i\leqslant 20}$ and $(p_i^L,\hat{\sigma}(p_i^L,L))_{0\leqslant i\leqslant 20}$. (These polynomials, essentially degree 11 least square fits, were arrived at through a combination of subjective and quantitative criteria—see Appendix.) We denote these polynomials, respectively, by $\tilde{X}^+(p,L)$ and $\tilde{\sigma}(p,L)$ (for each of the four L's, these are polynomial in p). The polynomials $\tilde{X}^+(p,200)$ and $\tilde{\sigma}(p,200)$ are plotted in Fig. 3.

Replacing $\hat{X}^+$ with $\tilde{X}^+$ and $\hat{\sigma}$ with $\tilde{\sigma}$ in (10), and defining the $\tilde{\epsilon}$'s again to produce equality, we obtain

$$\frac{\tilde{X}^+(p(s),L)}{\tilde{\sigma}(p(s),L)}=\frac{L^{\gamma/\nu}}{\tilde{\sigma}(p(s),L)}f(s)+\frac{L^{(\gamma/\nu)-\delta}}{\tilde{\sigma}(p(s),L)}g(s)+\tilde{\epsilon}(p_c,\gamma,\nu,\delta,f,g\,;s,L). \tag{12}$$

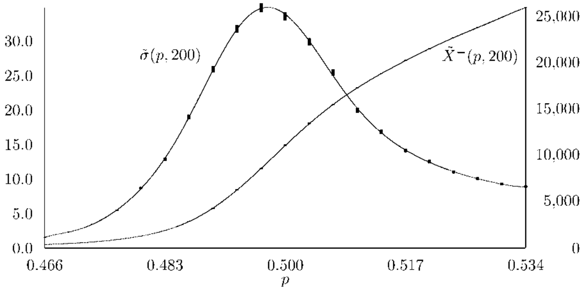

Fig. 3. $\tilde{X}^+(p,200)$ (scale on right axis) and $\tilde{\sigma}(p,200)$ (scale on left axis). Bars show 99% confidence intervals for $E\bar{X}^+(p,200)$ and $\sigma(p,200)$, based on the data.

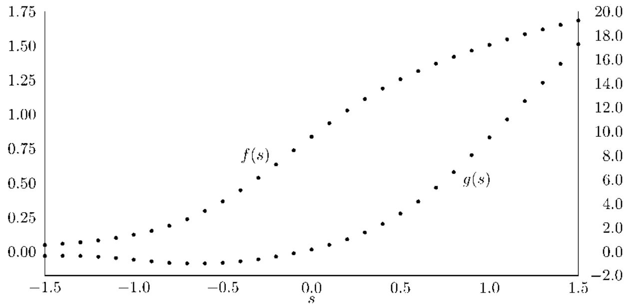

Fig. 4. $f|_S$ (scale on left axis) and $g|_S$ (scale on right axis).

For $L = 200$, 400, 600, and 800, and s ranging from -1.5 to 1.5 in steps of 0.1 (i.e., with $S = \{-1.5, -1.4, \ldots, +1.4, +1.5\}$), we numerically searched a fine grid of values for p_c, γ, ν, and δ and, given these quantities, used standard quadratic minimization techniques to find $f|_S$ and $g|_S$ with the objective of minimizing the quantity

$$\sum_{s \in S} \sum_{L} \tilde{\epsilon}(p_c, \gamma, \nu, \delta, f|_S, g|_S\, ; s, L)^2. \tag{13}$$

To three decimal places, the minimum value occurred with the following estimates of the true parameters: $\hat{p}_c = 0.500$, $\hat{\gamma} = 2.392$, $\hat{\nu} = 1.336$, and $\hat{\delta} = 0.946$. Figure 4 displays the corresponding values of $f(s)$ and $g(s)$ for $s \in S$.

We note that these results are not excessively sensitive to the degree, in this case 11, of the fitting polynomials. Table I reports the analogous estimates over a range of degrees (in each case we held p_c constant at 0.5 but allowed γ, ν, δ, $f|_S$, and $g|_S$ to optimize).

Table I. Minimizing Exponents Corresponding to Five Different Polynomial Fits of the Data

Polynomial degree	$\hat{\gamma}$	$\hat{\nu}$	$\hat{\delta}$
9	2.390	1.335	0.952
10	2.390	1.335	0.945
11	2.392	1.336	0.946
12	2.390	1.335	0.949
13	2.380	1.330	0.959

Phase Transition, Part 2. Based on the results of Part 1, we statistically test the hypothesis that $p_c^* = 1/2$, $\gamma^* = 43/18$, $\nu^* = 4/3$, and $\delta^* = 1$. To this end we ran a new, independent, set of data. This time we simulated the systems corresponding to values of L ranging from 200 to 800 in steps of 25 and for s taking on the values -1, 0, and $+1$ (or, equivalently for each L, for p taking on values $\frac{1}{2} - L^{-3/4}$, $\frac{1}{2}$, $\frac{1}{2} + L^{-3/4}$) for a total of 75 (s, L) pairs. The motivation for shifting from few values of L and many values of p (as in Part 1) to many values of L and few values of s (few values of p for each L) is that each value of s reduces the degrees of freedom by 2 since $f(s)$ and $g(s)$ are estimated parameters. This shift allows us $75 - 2 \times 3 = 69$ degrees of freedom. Note that in Part 1, we needed good estimates of $E\bar{X}^+(p, L)$ for many values of p because, for each L, the values of p corresponding to each s varied with p_c and ν—free parameters in Part 1.

With the exponents fixed, we used standard minimization techniques as before to find $f(s)$ and $g(s)$, for $s = -1, 0, 1$, that minimizes the sum

$$\sum_{s \in \{-1, 0, 1\}} \sum_{L} \epsilon(f(s), g(s)\,;\, s, L)^2, \tag{14}$$

where the error terms are defined by the relation:

$$\frac{\hat{X}_2^+(s, L)}{\hat{\sigma}_2(s, L)} = \frac{L^{43/24}}{\hat{\sigma}_2(s, L)} f(s) + \frac{L^{19/24}}{\hat{\sigma}_2(s, L)} g(s) + \epsilon(f(s), g(s); s, L). \tag{15}$$

The values of $\hat{X}_2^+(s, L)$ and $\hat{\sigma}_2(s, L)$, i.e., the second data set, are tabulated in the appendix. As in Part 1, the data are independent across the 75 different (s, L) pairs.

First, we use the chi-square goodness-of-fit test to test for standard normality of the errors ϵ as defined in (15). We divide the line into the standard normal deciles, i.e., define $-\infty = x_0 < x_1 < \cdots < x_9 < x_{10} = \infty$ by $P[x_{i-1} < \text{standard normal} \leqslant x_i] = 1/10$. We let Q_i denote the number of pairs (s, L) with $x_{i-1} < \epsilon(s, L) \leqslant x_i$ (for $1 \leqslant i \leqslant 10$), so we will have that

$$C \equiv \sum_{i=1}^{10} \frac{(Q_i - 7.5)^2}{7.5} \tag{16}$$

is drawn (roughly) from a chi-square distribution with 9 degrees of freedom. For our particular data, we have $C = 6.733$, with corresponding P-value $P[\chi^2(9) \geqslant 6.733] = 0.68$ indicating a good fit by this test.

The sample mean of the 75 errors was $\bar{\epsilon} = -0.002$, with sample variance $S_\epsilon^2 = 0.847$. Neither of these quantities would lead to the rejection of the hypotheses of standard normality of the errors with any reasonable level of significance. Additionally, assuming the model and exponent values are correct, the value of the sum in (14) should be distributed like $\chi^2(69)$. The data yielded 63.5, which is within one standard deviation of the expected value of 69.

4. SIMULATION RESULTS ON RATE OF FIXATION

In this section we study numerically the rate at which $\sigma(t) \to \sigma(\infty)$ as $t \to \infty$ when $p = 1/2$. Based on preliminary numerical evidence (reported in ref. 18) and on heuristic arguments, this rate was postulated in ref. 19 to be exponential. For p sufficiently close to zero or one, exponential fixation was proved on the homogeneous tree of degree three in ref. 18, and (at least) stretched-exponentially fast fixation was proved on $\mathbb{Z}^d$ in ref. 20 and on $\mathbb{H}$ in ref. 3.

Specifically, we simulate the Markov process on the patch $\mathbb{V}(40)$ and study when a specified site in this patch flips for the last time. Our specified site is $v_0 \equiv (-\frac{\sqrt{3}}{2}, -\frac{1}{2}) + 20\mathbf{u} + 20\mathbf{v}$, which is located essentially in the middle of the patch. Here we explicitly do not use periodic boundary conditions. Letting $\partial\mathbb{V}(40)$ denote those sites in $\mathbb{V}(40)$ at graphical distance either 1 or 2 from some site in $\mathbb{V}(40)^c$, for each simulation we run two cases: (1) where $\sigma_v(t) = +1$ for all t and all $v \in \partial\mathbb{V}(40)$ and (2) where $\sigma_v(t) = -1$ for all t and all $v \in \partial\mathbb{V}(40)$. For each simulation, in cases (1) and (2) the spin values at time zero in the interior, $(\sigma_v(0)\colon v \in \mathbb{V}(40) \setminus \partial\mathbb{V}(40))$, are i.i.d. with $P[\sigma_v(0) = +1] = P[\sigma_v(0) = -1] = 1/2$. Also, for each simulation, in cases (1) and (2) the dynamics are identical in the sense that the order in which sites are (randomly) selected for possible spin flips is the same. In each of the 3 million simulations performed, the case (1) and case (2) values of $\sigma_{v_0}(t)$ agreed for all t, indicating that we effectively sampled from the infinite system.

Recall that in implementing the dynamics, we randomly (with replacement) select sites in $\mathbb{V}(40)$ for possible spin flips, simulating the ringing of Poisson clocks. The statistic that this yields is the number N of clock rings on the patch $\mathbb{V}(40)$ until v_0 last flips. To convert this into a time with the proper distribution, we compute $T = \sum_{n=1}^{N} Y_n$, where the Y_n are independent exponential random variables of mean $1/|\mathbb{V}(40)|$.

Figure 5 shows a (logarithmic) plot of the empirical estimate F_t of the tail, $P[T > t]$, for the time T until last flip of v_0. The tail appears to fall off exponentially fast. In fact, a least squares fit of $\log P[T > t]$ of the form $\alpha - \beta t^c$ produces minimal fitting error over the data interval $5 \leqslant t \leqslant 25$ when, to two decimal places, $c = 1.01$. Figure 5 shows this fit.

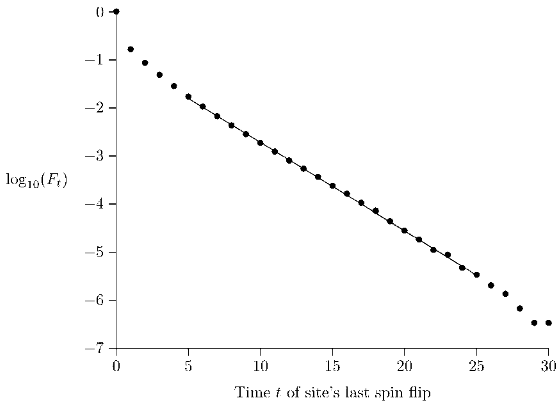

Fig. 5. Distribution of the time until site v_0 last flips, based on 3×10^6 simulations. Bullets • show $\log_{10}(F_t)$, where F_t is the fraction of simulations where the time of last flip at site v_0 exceeds t. Plot shows best linear fit of data for $5 \leqslant t \leqslant 25$.

APPENDIX A

A.1. Data for Phase Transition Part 1

The data for Phase Transition Part 1 is shown in Table II.

A.2. Polynomial Fitting of Data

The polynomials $\tilde{X}^+(p, L)$ of Section 3 are computed as follows. Recall that $\hat{\sigma}(p, L)$ is (an estimate of) the standard deviation of the estimator $\hat{X}^+(p, L)$. Then $\tilde{X}^+(p, L)$ is the degree 11 polynomial $P(p)$ that minimizes the quantity,

$$\sum_p \left[\frac{P(p) - \hat{X}^+(p, L)}{\hat{\sigma}(p, L)} \right]^2, \tag{17}$$

where p ranges over the 21 values shown above corresponding to the particular L. The choice of degree 11 was based on subjective criteria.

The polynomials $\tilde{\sigma}(p, L)$ are computed slightly differently. Let $\tilde{Q}(p)$ be the degree 11 polynomial $Q(p)$ that minimizes the quantity,

$$\sum_p \left[\frac{Q(p) - \hat{\sigma}^{1/2}(p, L)}{\hat{\sigma}^{1/2}(p, L)} \right]^2; \tag{18}$$

then take $\tilde{\sigma}(p, L) = \tilde{Q}(p)^2$. The decision to initially fit $\hat{\sigma}^{1/2}(p, L)$, rather than fit $\hat{\sigma}(p, L)$ directly, was again based on subjective criteria.

Table II. Data Is Based on 10000 Simulations for Each (p, L) Pair

p	$\hat{X}^{+}(p, L)$	$\hat{\sigma}(p, L)$	p	$\hat{X}^{+}(p, L)$	$\hat{\sigma}(p, L)$
	$L = 200$			$L = 400$	
0.4660	383.9	1.561	0.4801	1437.5	6.064
0.4694	502.6	2.334	0.4821	1839.0	8.112
0.4728	667.9	3.482	0.4841	2460.3	13.234
0.4762	923.2	5.497	0.4861	3360.6	19.643
0.4796	1315.5	8.713	0.4880	4752.7	30.340
0.4830	1912.6	12.869	0.4900	6933.5	46.514
0.4864	2887.7	19.019	0.4920	10345.5	67.322
0.4898	4324.4	25.944	0.4940	15503.5	91.839
0.4932	6318.9	31.773	0.4960	22051.7	110.983
0.4966	8625.7	34.837	0.4980	30179.4	122.134
0.5000	11157.5	33.568	0.5000	38561.6	118.090
0.5034	13535.4	29.888	0.5020	46505.7	103.189
0.5068	15545.2	25.467	0.5040	53427.6	84.674
0.5102	17393.6	19.938	0.5060	59392.6	67.733
0.5136	18932.7	16.814	0.5080	64382.2	54.219
0.5170	20355.7	14.151	0.5100	68667.3	45.935
0.5204	21615.5	12.529	0.5120	72666.0	38.588
0.5238	22824.3	11.025	0.5139	76260.7	34.150
0.5272	23928.6	10.085	0.5159	79630.3	30.071
0.5306	25025.1	9.273	0.5179	82740.0	27.414
0.5340	26072.1	8.924	0.5199	85736.3	25.084
	$L = 600$			$L = 800$	
0.4854	3043.1	12.342	0.4883	5181.5	20.723
0.4869	3938.0	18.370	0.4895	6745.7	31.483
0.4883	5214.9	27.622	0.4906	8902.0	46.830
0.4898	7130.7	41.376	0.4918	12157.9	71.621
0.4912	10137.9	65.065	0.4930	17196.1	109.773
0.4927	14931.9	99.250	0.4942	24866.4	164.613
0.4942	22039.3	144.828	0.4953	36909.0	239.188
0.4956	32148.3	190.745	0.4965	54497.2	323.397
0.4971	46304.4	230.259	0.4977	77311.8	386.662
0.4985	62314.1	247.714	0.4988	104328.3	418.226
0.5000	80426.6	239.863	0.5000	133529.4	408.751
0.5015	95927.5	209.643	0.5012	160275.1	353.765
0.5029	110088.6	176.674	0.5023	183768.3	292.729
0.5044	121686.3	144.172	0.5035	203313.7	236.978
0.5058	132168.6	110.968	0.5047	219947.2	187.504
0.5073	140761.7	93.133	0.5058	234400.6	156.161
0.5088	148472.7	79.718	0.5070	247200.0	130.098
0.5102	155501.2	68.704	0.5082	258578.2	115.031
0.5117	162028.2	61.271	0.5094	269327.8	98.169
0.5131	168165.2	53.831	0.5105	278977.8	88.767
0.5146	173958.2	49.415	0.5117	288303.1	80.756

Table III. Data Is Based on 17197 Simulations for Each (−1, L) and (0, L) Pair, and 14173 Simulations for Each (+1, L) Pair

	$s=-1$		$s=0$		$s=+1$	
L	$\hat{X}^+(s, L)$	$\hat{\sigma}(s, L)$	$\hat{X}^+(s, L)$	$\hat{\sigma}(s, L)$	$\hat{X}^+(s, L)$	$\hat{\sigma}(s, L)$
200	1560.7	7.898	11097.7	25.973	21018.8	11.020
225	1948.3	9.951	13701.4	32.226	25839.2	13.339
250	2369.3	12.014	16591.4	38.868	31082.0	15.780
275	2793.7	14.107	19650.5	45.822	36738.4	18.744
300	3301.9	16.938	22954.3	53.430	42823.0	21.306
325	3772.3	18.809	26577.1	61.794	49327.9	24.335
350	4315.2	21.889	30336.8	70.921	56149.4	27.911
375	4950.8	24.938	34365.2	79.086	63458.7	31.885
400	5486.4	27.482	38652.3	88.809	71108.7	34.557
425	6144.8	30.335	42912.9	100.058	79184.4	38.645
450	6846.8	35.045	47647.5	110.802	87691.6	42.280
475	7459.4	36.827	52502.9	120.892	96425.0	47.108
500	8246.1	41.243	57742.7	131.947	105643.8	51.435
525	9022.9	44.396	62935.9	144.758	115055.4	55.918
550	9896.3	49.697	68113.1	157.782	124961.6	59.946
575	10666.7	53.644	73714.5	170.714	135329.2	65.212
600	11470.4	57.073	79882.0	184.482	146035.0	69.404
625	12448.3	62.874	85709.0	198.823	156839.7	75.573
650	13274.2	65.955	91887.1	213.929	168251.3	80.729
675	14234.0	72.213	98483.6	227.318	179879.7	86.758
700	15176.6	75.725	105012.8	241.510	191865.3	92.764
725	16092.2	80.443	111677.4	256.731	204087.2	98.596
750	17250.0	87.445	118916.6	273.585	216988.8	103.925
775	18171.5	90.896	126008.6	292.703	229813.8	110.130
800	19144.0	94.206	133041.9	309.130	243476.7	112.770

A.3. Data for Phase Transition Part 2

The data for Phase Transition Part 2 is shown in Table III.

ACKNOWLEDGMENTS

We thank Alan Sokal for very useful discussions and advice about finite-size scaling. We also note the participation of Elizabeth Zollinger as part of an undergraduate research experience supported by the NSF VIGRE program. Research of C.D.H. supported in part by NSF Grants DMS-98-15226 and DMS-02-03943 and by a Eugene Lang Research Fellowship. Research of C.M.N. supported in part by NSF Grants DMS-98-03267 and DMS-01-04278.

REFERENCES

1. A. J. Bray, Theory of phase-ordering kinetics, *Adv. Phys.* **43**:357–459 (1994).
2. T. M. Liggett, *Interacting Particle Systems* (Springer, New York, 1985).
3. F. Camia, C. M. Newman, and V. Sidoravicius, Approach to fixation for zero-temperature stochastic Ising models on the hexagonal lattice, in *In and Out of Equilibrium: Probability with a Physics Flavor*, V. Sidoravicius, ed. (Birkhäuser, Boston, 2002), pp. 163–183.
4. S. Nanda, C. M. Newman, and D. L. Stein, Dynamics of Ising spin systems at zero temperature, in *On Dobrushin's Way (From Probability Theory to Statistical Physics)*, R. Minlos, S. Shlosman, and Y. Suhov, eds., *Amer. Math. Society Transl. (2)* **198**:183–194 (2000).
5. H. Kesten, *Percolation Theory for Mathematicians* (Birkhäuser, Boston, 1982).
6. F. Camia, E. De Santis, and C. M. Newman, Clusters and recurrence in the two-dimensional zero-temperature stochastic Ising model, *Ann. Appl. Probab.* **12**:565–580 (2002).
7. T. E. Harris, A correlation inequality for Markov processes in partially ordered state spaces, *Ann. Probab.* **5**:451–454 (1977).
8. A. Gandolfi, M. Keane, and L. Russo, On the uniqueness of the infinite occupied cluster in dependent two-dimensional site percolation, *Ann. Probab.* **16**:1147–1157 (1988).
9. M. P. M. den Nijs, A relation between the temperature exponents of the eight-vertex and q-state Potts model, *J. Phys. A: Math. Gen.* **12**:1857–1868 (1979).
10. B. Nienhuis, E. K. Riedel, and M. Schick, Magnetic exponents of the two dimensional q-state Potts model, *J. Phys. A: Math. Gen.* **13**:L189–L192 (1980).
11. R. P. Pearson, Conjecture for the extended Potts model magnetic eigenvalue, *Phys. Rev. B* **22**:2579–2580 (1980).
12. G. Grimmett, *Percolation* (Springer, Berlin, 1999).
13. L. Russo, A note on percolation, *Z. Wahrsch. Verw. Gebiete* **43**:39–48 (1987).
14. H. Saleur and B. Derrida, A combination of Monte Carlo and transfer matrix methods to study $2d$ and $3d$ percolation, *J. Physique* **46**:1043–1057 (1985).
15. M. N. Barber, Finite size scaling, in *Phase Transitions and Critical Phenomena*, Vol. 8, C. Domb and J. L. Lebowitz, eds. (Academic, London, 1983), pp. 146–266.
16. J. L. Cardy, ed., *Finite-Size Scaling* (North-Holland, Amsterdam, 1988).
17. V. Privman, ed., *Finite Size Scaling and Numerical Simulation of Statistical Systems* (World Scientific, Singapore, 1990).
18. C. D. Howard, Zero-temperature Ising spin dynamics on the homogeneous tree of degree three, *J. Appl. Probab.* **37**:736–747 (2000).
19. C. M. Newman and D. L. Stein, Blocking and persistence in the zero-temperature dynamics of homogeneous and disordered Ising models, *Phys. Rev. Lett.* **82**:3944–3947 (1999).
20. L. R. Fontes, R. H. Schonmann, and V. Sidoravicius, Stretched exponential fixation in stochastic Ising models at zero temperature, *Commun. Math. Phys.* **228**:495–518 (2002).